Effects of Intra- and Intersubunit Hydrogen Bonds on the R–T Transition in Human Hemoglobin As Studied with α42(C7) and β145(HC2) Mutations†

Akiko Togi, Koichiro Ishimori, Masashi Unno, Takashi Konno, and Isao Morishima*

Division of Molecular Engineering, Graduate School of Engineering, Kyoto University, Kyoto 606-01, Japan

Gentaro Miyazaki

Department of Biophysical Engineering, Faculty of Engineering Science, Osaka University, Toyonaka, Osaka 560, Japan

Kiyohiro Imai

Department of Physicochemical Physiology, Medical School, Osaka University, Suita, Osaka 565, Japan

Received February 22, 1993; Revised Manuscript Received June 2, 1993®

ABSTRACT: To clarify the effects of specific inter- and intrasubunit hydrogen bonds on the R–T transition in human hemoglobin (Hb A), the recombination reaction of carbon monoxide with artificial mutant Hbs was measured and analyzed. One of the hydrogen bonds we focused on is formed between Tyr-42α and Asp-99β in the α1–β2 interface of Hb A, which is one of the hydrogen bonds characteristic of the T state. Hb His-42α, in which Tyr-42α is replaced by His to perturb this hydrogen bond, showed that the ligand-free R to T transition rate was decreased by 20-fold compared with that for Hb A. This mutation caused the destabilization of the transition state in the R to T quaternary structure change by about 7 kJ mol^{-1}, indicating that the hydrogen bond between Tyr-42α and Asp-99β plays a definite role in the R–T transition as well as in stabilization of the equilibrium T state. Hb Phe-145β, in which Tyr-145β is replaced by Phe and the intrasubunit hydrogen bond between Tyr-145β and Val-98β is lacking, also showed a slow R–T transition rate as observed in Hb His-42α. The published crystallographic data suggest that this intrasubunit hydrogen bond stabilizes the transition state by reducing the freedom of motion of the C-terminus of the β subunit and, thereby, facilitates the R–T transition.

Upon oxygenation or deoxygenation, human hemoglobin A (Hb A) undergoes structural changes including a global rearrangement of the intra- and intersubunit hydrogen bonds (Perutz, 1970; Baldwin & Chothia, 1979; Perutz et al., 1987). In such structural changes, the symmetrically related αβ dimers rotate by about 15° relative to each other, resulting in atomic displacements as large as 6 Å at the intersubunit contacts (Baldwin & Chothia, 1979). Several natural mutants having amino acid substitutions at the subunit interface have been studied to gain an insight into the molecular mechanism of cooperativity in oxygenation of Hb. The usefulness of naturally occurring point mutants, however, is restricted by limited availability of material and limited number of existing substitutions (Imai et al., 1989). Previously, using genetic engineering techniques, we synthesized several mutant Hbs and investigated the effects of the hydrogen bonds located at the α1–β2 subunit interface or within the subunit on the stability of the static tertiary and quaternary structures of Hb (Imai et al., 1991; Ishimori et al., 1992). Our oxygen equilibrium, UV-absorption spectrum, proton NMR spectrum, and resonance Raman scattering data not only confirmed the roles of specific hydrogen bonds previously predicted from crystallographic data but also provided information regarding some stereochemical effects of the amino acid side chains participating in the hydrogen bonds.

In spite of the accumulation of information about the static and equilibrium state of the mutant Hbs, little is known about the effect of the hydrogen bonds on the dynamic process in oxygenation. In the present study, we will describe carbon monoxide recombination kinetics of artificial mutant Hbs and the effects of the hydrogen bonds on the R–T transition dynamics. The mutant Hbs prepared are Hb Phe-42α (Tyr-42α → Phe) and Hb His-42α (Tyr-42α → His), in which the intersubunit hydrogen bond between Tyr-42α and Asp-99β is absent and weakened, respectively, and Hb Phe-145β (Tyr-145β → Phe), which lacks the intrasubunit hydrogen bond formed between Tyr-145β and the carbonyl group of Val-98β. Of all the hydrogen bonds existing in the Hb tetramer, these *inter*subunit hydrogen bonds and the *intra*subunit hydrogen bond have been considered to serve as key interactions contributing to the allosteric transition through studies using natural and artificial mutants (Jones et al., 1967; Reed et al., 1966; Weatherall et al., 1977; Charache et al., 1975; Winslow et al., 1976; Imai et al., 1991; Ishimori et al., 1992). Using these mutants, we performed laser-photolysis experiments (Gibson, 1959; Gray, 1975; Sawicki & Gibson, 1976, 1977; Sawicki & Khaleque, 1983; Vandegriff et al., 1991) combined with the "two-state model" simulation (Monod et al., 1965) and obtained the R–T transition rates of those mutants as well as wild-type Hb. On the basis of transition-state theory, we will try to clarify the effects of hydrogen bonding on the R–T transition dynamics.

MATERIALS AND METHODS

Preparation of Hemoglobins. Human Hb A was prepared from whole blood by a standard method (Ishimori & Morishima, 1988). Mutant Hbs were expressed in *Escherichia*

† This work was supported in part by Grants 03241103 and 03780152 from the Ministry of Education, Science and Culture of Japan (to I.M. and K. Ishimori). K. Imai was supported by Ajinomoto Co. (Tokyo).

* To whom correspondence should be addressed.

® Abstract published in *Advance ACS Abstracts,* September 1, 1993.

0006-2960/93/0432-10165$04.00/0

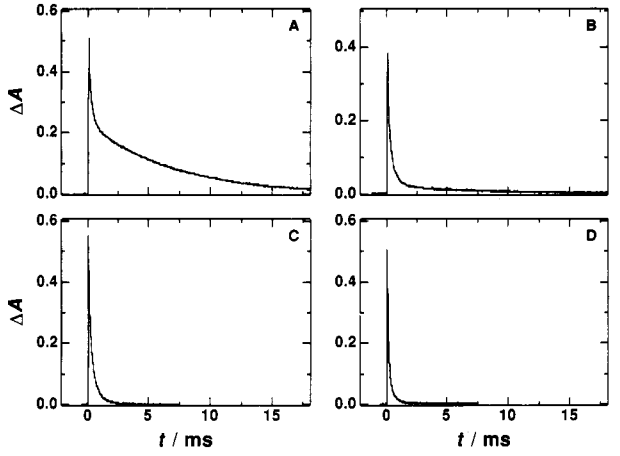

FIGURE 1: Millisecond time courses for the recombination of ~0.5–0.7 mM CO with native and mutant Hbs: (A) Hb A, (B) Hb Phe-145β, (C) Hb His-42α, and (D) Hb Phe-42α. The reactions were carried out at 20 °C and pH 7 in 50 mM Tris–0.1 M Cl^- buffer and were monitored at 436 nm. Protein concentrations were (A) 103, (B) 101, (C) 100, and (D) 103 μM on a heme basis, and CO concentrations were (A) 0.63, (B) 0.56, (C) 0.58, and (D) 0.54 mM.

coli from a synthetic gene according to Nagai et al. (1985) and purified to homogeneity as described by Imai et al. (1991) and Ishimori et al. (1992). All experiments were carried out at 20 °C in 50 mM Tris–0.1 M Cl^-, pH 7.0.

Kinetic Measurements. Bimolecular association rate constants were determined by flash photolysis using a pulsed dye laser system and an apparatus consisting of a photographic strobe unit (Sunpack Auto 622), whose pulse width was ~0.5 ms. Details of the apparatus were described previously (Unno et al., 1990). In order to minimize dimer formation, 1-mm path length cells and high concentrations of protein samples [~100 μM (heme)] were used. The sample cell was placed at a 45° angle to the excitation source and the absorbance spectra were monitored at right angles to the excitation light. The monitoring wavelength was 436 nm, which is an isosbestic point for the R- and T-state Hb.[1] The association rate constants for the R-state molecular species were obtained from the partial photolysis technique (<10% photolysis) by the laser system. The half-peak duration of the excitation pulse (300 ns) is short enough to measure the R to T transition rate (Sawicki & Gibson, 1976; Hofrichter et al., 1983; Mathews et al., 1989). To the observed time courses was fitted a two-exponential expression with equal amplitudes for the two phases (Mathews et al., 1989).

In the case of CO rebinding to the T-state species, ~40% photolysis was performed by the photographic strobe unit. The time courses were simulated by a single exponential in the time range of ~4–18 ms. In the R and T state of the mutants, the residuals of the observed time course minus the best-fit exponential line exhibit a random distribution about a mean value of zero (data not shown), indicating the time courses for the mutants can be simulated by the same exponential expressions as for native Hb A.

Formulation of Two-State Model. Equations 1–7 present the formulations of the two-state model used in the present study:

$$\mathrm{Hb_R}(\alpha_m\beta_n) \xrightarrow{k(\mathrm{R}\alpha)} \mathrm{Hb_R}(\alpha_{m+1}\beta_n) \quad (1)$$

$$\mathrm{Hb_R}(\alpha_n\beta_m) \xrightarrow{k(\mathrm{R}\beta)} \mathrm{Hb_R}(\alpha_n\beta_{m+1}) \quad (2)$$

$$\mathrm{Hb_T}(\alpha_m\beta_n) \xrightarrow{k(\mathrm{T})} \mathrm{Hb_T}(\alpha_{m+1}\beta_n) \quad (3)$$

$$\mathrm{Hb_T}(\alpha_n\beta_m) \xrightarrow{k(T)} \mathrm{Hb_T}(\alpha_n\beta_{m+1}) \quad (4)$$

$$\mathrm{Hb_R}(\alpha_p\beta_q) \underset{K_0/L(cd)^{p+q}}{\overset{K_0/d^{p+q}}{\rightleftharpoons}} \mathrm{Hb_T}(\alpha_p\beta_q) \quad (5)$$

$$\mathrm{D}(\alpha_0\beta_m) \xrightarrow{k(\mathrm{R}\alpha)} \mathrm{D}(\alpha_1\beta_m) \quad (6)$$

$$\mathrm{D}(\alpha_m\beta_0) \xrightarrow{k(\mathrm{R}\beta)} \mathrm{D}(\alpha_m\beta_1) \quad (7)$$

$$0 \le m \le 1 \quad 0 \le n \le 2 \quad 0 \le p \le 2 \quad 0 \le q \le 2$$

This model, which includes dimerization, has proved to be useful in the study of reactions of CO and O_2 with Hb (Sawicki & Gibson, 1976, 1977; Sawicki & Khaleque, 1983; Vandegriff et al., 1991). In the simulation, we partially took into account the chain difference, because the CO rebinding rate constant for only the R-state Hb can be obtained separately for the α and β subunits. In eqs 1–4, $\mathrm{Hb_R}(\alpha_m\beta_n)$ and $\mathrm{Hb_T}(\alpha_m\beta_n)$ represent R- and T-state Hbs with $(m+n)$ bound CO molecules, and $k(\mathrm{R}\alpha)$, $k(\mathrm{R}\beta)$, and $k(\mathrm{T})$ denote the rate constants for CO rebinding to the α and β subunits of the R-state Hb and to the T-state Hb, respectively. Thermal dissociation of CO from Hb during the CO rebinding reaction (Sharma et al., 1976) and the dimer reassociation following photolysis (Kellett & Gutfreund, 1970; Wiedermann & Olson, 1975) were neglected, since they are too slow to contribute to the observed kinetics in the present experiments. The transition changes between the R and T quaternary structures is represented by eq 5. L and c, respectively, are the equilibrium constant between unliganded R_0 and T_0 and the ratio of the ligand association equilibrium constant for the T state to that for the R state. K_0 is the rate of the conformational change from unliganded R state (R_0) to unliganded T state (T_0). R_0 to T_0 conformational change rate is reduced by a factor d at each ligand binding to the R-state. CO binding to dimers at the R-state rate is represented by eqs 6 and 7. $\mathrm{D}(\alpha_m\beta_n)$ represents the dimer species with $(m+n)$ bound CO molecules. We also assumed that the quantum efficiencies of the α and β subunit in Hb tetramer are the same, since those of the isolated α and β chains were approximately the same (Hofrichter et al., 1985), and that the quantum efficiency is independent of the degree of photolysis. Thus, partial photolysis was assumed to produce a binomial distribution of the intermediates.

RESULTS

Time Courses for CO Recombination with Native and Mutant Hemoglobins. Typical time courses of 436-nm absorption for the CO recombination with Hb A, Hb Phe-145β, Hb His-42α, and Hb Phe-42α after ~50–60% laser photolysis are shown in Figure 1, panels A–D, respectively. It is well documented that the initial portions of the time course (0– ~1 ms) correspond to the CO recombination to the R-state Hb and the slower relaxations (~1–18 ms) result from recombination to the T-state Hb (Gibson, 1959; Antonini

[1] To provide more direct access to the kinetics of the R–T transition, we tried to measure kinetics at other wavelengths. For example, we also used 425 nm, an isosbestic point for the spectral change between deoxy R-state Hb and carbonmonoxy R-state Hb, so that we could estimate the R–T transition rate directly. However, we failed to get any reliable data by measuring kinetics at such other wavelengths since the fraction of the T-state was too small to simulate in our mutant hemoglobins.

Table I: Typical Empirical Parameters for CO Bimolecular Association with Hb A, Hb Phe-145β, Hb His-42α, and Hb Phe-42α[a]

	k_{on} (M^{-1} s^{-1})		
	R state		
	α subunit	β subunit	T state
Hb A	$(4.54 \pm 0.06) \times 10^6$	$(1.29 \pm 0.02) \times 10^7$	$(2.39 \pm 0.02) \times 10^5$
Hb His-42α	$(3.32 \pm 0.01) \times 10^6$	$(1.11 \pm 0.01) \times 10^7$	[b]
Hb Phe-42α	$(3.40 \pm 0.34) \times 10^6$	$(1.10 \pm 0.11) \times 10^7$	[b]
Hb Phe-145β	$(4.84 \pm 0.09) \times 10^6$	$(1.33 \pm 0.05) \times 10^7$	$(2.70 \pm 0.32) \times 10^5$

[a] Experiments were performed with a millisecond laser photolysis apparatus in 50 mM Tris–0.1 M Cl^-, pH 7, at 20 °C. The rate constants of the R-state Hb were evaluated by simulating the observed absorbance traces with a biexponential expression, and the rate constants of the T-state Hb were evaluated by simulation with a single-exponntial expression as described in the text. The values listed represent the average of fits to five runs. Each run is an average of 3–10 laser shots. The errors listed are the standard deviation from the mean. [b] The rate constants of the T state for Hb His-42α and Hb Phe-42α could not be determined since the fraction of the T-state Hb was too small in both mutants.

& Brunori, 1971; Antonini et al., 1972; Schmelzer et al., 1972). The most characteristic feature of the time courses of the mutants as compared with that of Hb A is the remarkable decrease in the slow component, which corresponds to CO recombination to the T-state Hb. Hb Phe-42α has almost no fraction of the slow component. Such a drastic decrease in the slower kinetic component was also encountered in CO binding kinetics of viscous solution systems (Sawicki & Khaleque, 1983). By fitting the two-state model (Monod et al., 1965) to their kinetic data, they concluded that the decrease of the slow fraction was caused by a slower R to T transition rate. Findsen et al. (1988) also supported this view by their time-resolved resonance Raman spectra measurements in glycerol solution systems. Thus, the present mutational effect observed by us could also be caused by the reduced R-to-T transition rates for the mutants. To confirm the change in the R–T transition rates, we carried out two-state model fitting to the time courses at 436 nm.

Simulations and Parameters. The differential equations derived from eqs 1–7 were iteratively solved by using Euler's numerical method at 1-μs intervals with a digital computer, giving appropriate parameter values and simulated rebinding curves.[2] In Table II are shown the values of L and c for Hb A and the mutant Hbs, which were obtained from our oxygen equilibrium curve measurements (Imai et al., 1991; Ishimori et al., 1992). The tetramer–dimer dissociation constant $K_{4,2}$ was set to be 3 μM for Hb A (Andrews, 1964; Kellet, 1971; Chu & Ackers, 1981) and Hb Phe-145β, and 79 μM for Hb His-42α and Hb Phe-42α.[3] The CO binding rate for the R- and T-state Hbs [k(Rα), k(Rβ), and k(T)] were determined experimentally in the present study (Table I). As the parameter d for Hb A and the mutant Hbs, we adopt the value of 2.5,[4] which was used in some previous studies (Sawicki & Gibson, 1976; Sawicki & Khaleque, 1983). Thus, only one free parameter, K_0, was set variable to obtain the best fit in the model calculations to the experimental rebinding data.

Simulations for R to T Transition. Figure 2 shows the results of simulations for Hb His-42α and Hb Phe-145β. For Hb Phe-42α, however, the thermodynamic properties were so different from those of Hb A that we could not determine the R–T transition rate. For Hb A, the best-fit value of K_0 was 1.9×10^4 s^{-1} (Table II), which corresponds to 53 μs as a lifetime and is in good agreement with the previous results (Vandegriff et al., 1991; Hofrichter et al., 1983; Murray et al., 1988; Su et al., 1989; Kaminaka et al., 1990).

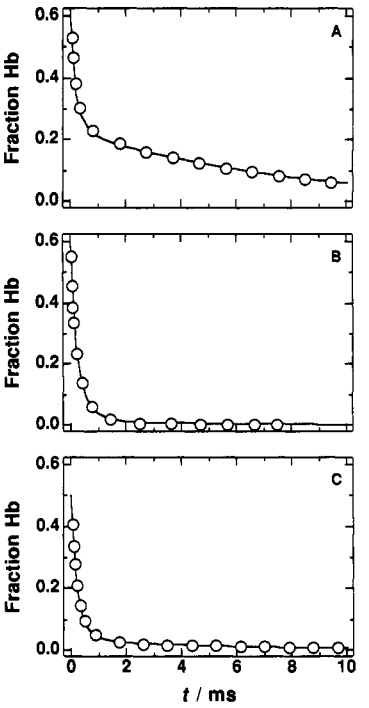

FIGURE 2: Open circles are data points of 436-nm absorption for Hb A (A), Hb His-42α (B), and Hb Phe-145β (C) depicted in Figure 1. The solid curves were calculated from the best-fit parameter values for the two-state model (Table II).

Table II: Best-Fit Parameter Values for Two-State Model Simulation and for Native and Mutant Hemoglobins[a]

	L[b]	c[b,c]	d[d]	$K_{4,2}$[a] (μM)	$K_0 \times 10^{-3}$[f] (s^{-1})
Hb A	1.5×10^6	0.0045	2.5	3	19
Hb His-42α	9.0×10^2	0.07	2.5	79	1
Hb Phe-42α	2.9	0.42	2.5	79	[g]
Hb Phe-145β	7.0×10^6	0.008	2.5	3	2

[a] Experimental conditions are as in Figure 1. The values of k(Ra), k(Rβ), and k(T) used for simulations were determined by multiplying the average values of k_{on} represented in Table I by the CO concentrations given in Figure 1. The values of k(T) could not be determined because of too-small fractions of the T-state in both Hb His-42α and Hb Phe-42α. For simulations of the two mutants, the k(T) obtained for Hb A was used instead. [b] From values of our oxygen equilibrium curve measured in 50 mM bis-Tris containing 0.1 M Cl^-, pH 6.8–6.9, at 25 °C (Imai et al., 1991; Ishimori et al., 1992). [c] The values of c were obtained as $c = K_T/K_R$. K_T and K_R are oxygen association equilibrium constants for the T-state and R-state Hbs, respectively. [d] See text. [e] Determined by gel filtration method (see text). [f] See text. [g] The best-fit values could not be obtained because of the large change in the equilibrium properties for Hb Phe-42α (see text).

[2] Numerical integration with time intervals less than 1 μs gave the same results.

[3] H. Morimoto, K. Imai, G. Fushitani, K. Miyazaki, K. Ishimori, and I. Morishima, unpublished data.

[4] The d value which is the linkage factor to estimate K_0 in this two-state model is presumptive and we were not able to exclude the possibility that other d values fit the time course data. In fact, we were able to get the reasonable fits in the model calculations to the experimental rebinding data with the K_0 value fixed and the d value variable. In this case, the d value was allowed to become as large as 50. It is unlikely that Hb His-42α and Hb Phe-145β exhibit such a large d value because these mutants showed mild structural and functional defects as previously reported (Ishimori et al., 1989, 1992; Imai et al., 1991). It was also confirmed that small deviations in the d value (e.g., from 2.5 to 5) resulted in slight changes in the K_0 value.

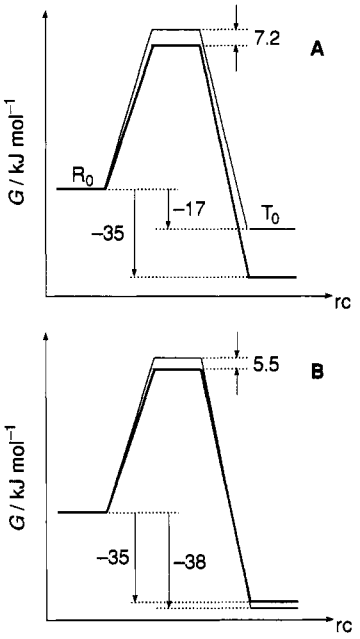

FIGURE 3: Free energy diagrams for the R_0 to T_0 transition of Hb His-42α (A) and Hb Phe-145β (B) (thin lines) compared with that of Hb A (thick lines) plotted versus the reaction coordinate for the R_0 to T_0 transition. The free energy differences between unliganded R_0 and T_0 states were calculated from eq 8. The differences of the free energy at the transition state between Hb A and the mutant Hbs were calculated from eq 9.

In the simulation of Hb His-42α, at first we fixed the value of K_0 to that obtained for Hb A (1.9×10^4 s^{-1}) and adopted the values of L, c, and $K_{4,2}$ in Hb His-42α. The calculated curve was not able to simulate the data points of Hb His-42α, indicating that the major differences in the time courses between Hb A and Hb His-42α cannot be accounted for by the differences in the equilibrium properties. To obtain reasonable fitting, we varied K_0 and obtained 1×10^3 s^{-1} as a best-fit value (Figure 2B and Table II). On the other hand, Hb Phe-145β has equilibrium parameter values which are quite similar to those of Hb A (Table II). Simulations were performed by varying the value of K_0 and a best-fit value of $K_0 = 2 \times 10^3$ s^{-1} was obtained (Figure 2C and Table II).

Effects of the Hydrogen Bonds on the R–T Transition. Based on K_0 and L in Table II, free-energy diagrams for the R_0–T_0 transition of Hb His-42α and Hb Phe-145β as compared with Hb A are drawn schematically in Figure 3, panels A and B, respectively, where the free energy of the system is depicted as a function of the reaction coordinate of the R_0 to T_0 transition. Bold lines represent the free-energy diagram for Hb A, and thin lines are for the mutant Hbs. The free energy of the R state is used as a reference state because the previous spectroscopic studies indicated that the R-state structure of the mutant Hbs is similar to that of Hb A (Imai et al., 1991; Ishimori et al., 1992).[5] The difference in the free energy between R_0 and T_0 (ΔG_{R-T}) for each Hb was calculated from the allosteric constant L as

$$\Delta G_{R-T} = -RT \ln L \quad (8)$$

where R is the gas constant and 293.15 K was used for the temperature T. The free-energy barrier at the R_0 to T_0 transition ($\Delta G^{\ddagger}_{R\rightarrow T}$) is given by

$$\Delta G^{\ddagger}_{R\rightarrow T} = -RT \ln (K_0/\nu) \quad (9)$$

where ν is the preexponential factor (Glasstone et al., 1941). As we are only interested in relative changes in the $\Delta G^{\ddagger}_{R\rightarrow T}$ by mutations, an absolute value of ν is not important. For Hb His-42α and Hb Phe-145β, about 20-fold and 10-fold decreases in K_0 as compared with Hb A (Table II) correspond to about 7.2 and 5.5 kJ mol^{-1} rises in $\Delta G^{\ddagger}_{R\rightarrow T}$, respectively (Figure 3A).

DISCUSSION

Effects of the Hydrogen Bond between Tyr-42α and Asp-99β. In previous studies of natural and artificial mutant Hbs (Jones et al., 1967; Reed et al., 1966; Weatherall et al., 1977; Imai et al., 1991; Ishimori et al., 1992), the hydrogen bond between Tyr-42α and Asp-99β has been proved to be crucial for cooperative oxygen binding. The complete lack of the slow CO-rebinding component in Hb Phe-42α indicates that the breakage of this hydrogen bond prevents the R-state Hb from converting into the T state due to the remarkable destabilization of the T state and/or the transition state between the R and T states. The degree of destabilization in the T state was estimated as 28 kJ mol^{-1} by eq 8. However, the stability of the transition state remains unknown because we were not able to measure the R–T transition rate of Hb Phe-42α.

Our previous paper (Imai et al., 1991) reported that Hb His-42α exhibited mild functional and structural defects, which are ascribed to a perturbed hydrogen bond formed between His-42α and Asp-99β in the deoxy state. Figure 3A shows that the mutation α42Tyr → His also destabilizes the T-state Hb by 17 kJ mol^{-1}, suggesting that the T state of Hb His-42α is more stabilized than that of Hb Phe-42α by the hydrogen bond between His-42α and Asp-99β. In the transition state, about a 7.2 kJ mol^{-1} rise in $\Delta G^{\ddagger}_{R\rightarrow T}$ (Figure 3A) was observed. The observed changes in $\Delta G^{\ddagger}_{R\rightarrow T}$ for Hb His-42α can be attributed to a mutational impairment of the hydrogen bond in the transition state. These considerations lead us to the conclusion that the hydrogen bond between Tyr-42α and Asp-99β exerts a stabilization effect on the transition state. In other words, since the free energy contribution of one hydrogen bond in protein systems is estimated as 4–8 kJ mol^{-1} (Perutz, 1970; Fersht et al., 1985), the hydrogen bond between Tyr-42α and Asp-99β is probably formed at the transition state in about a half degree compared with the equilibrium T-state.

Eaton and co-workers (Hofrichter et al., 1991; Eaton et al., 1991) suggested that the transition state for the R to T quaternary structure change has much more R-like than T-like thermodynamic properties. In our study, the perturbation of the T-state-specific hydrogen bonds located at the subunit interface affected the stability of the transition state for the R to T structural change. Our study also indicates that the quaternary structure of the transition state as watched at the subunit interface is more or less T-like structure as far as the hydrogen bonding is concerned.

Effects of the Hydrogen Bonds between Tyr-145β and Val-98β. The 145β natural mutants which have been discovered to date fail to retain the T-state conformation in the deoxygenated form, resulting in high oxygen affinities and diminished cooperativity (Charache et al., 1975; Winslow et al., 1976). For our mutant, Hb Phe-145β, in which the intrasubunit hydrogen bond is absent, the T-state is almostas stable as that for Hb A (Figure 3B). Further, the replacement of the Tyr with Phe did not drastically affect the equilibrium function and the static structure of Hb (Ishimori et al., 1992).

[5] In Phe-145β, since the intrasubunit hydrogen bond is ruptured in the oxygenated state as well as in the deoxygenated state, this breakage might cause destabilization in the equilibrium R state.

The free energy loss caused by the rupture of the hydrogen bonds is probably compensated by some interaction involving the benzene ring of Phe-145β as suggested in our previous paper (Ishimori et al., 1992).

However, the time course of the CO rebinding to Hb Phe-145β is quite different from that to Hb A. This mutant Hb showed about a 10-fold decrease in K_0 compared with the K_0 value for Hb A (Table II). This decrease in K_0 corresponds to about a 5.5 kJ mol^{-1} rise in $\Delta G^{\ddagger}_{R\rightarrow T}$ (Figure 3A). The loss of the stabilization energy of the R–T transition in Hb Phe-145β is close to that in Hb His-42α, implying that the hydrogen bond between Tyr-145β and Val-98β also contributes to the stabilization of the transition state between the R and T states.

The crystallographic data for Hb A provide a more precise picture of the effects of the hydrogen bonds on the transition state. According to the refined crystal structure of oxygenated Hb (Shaanan, 1983), Tyr-145β is hydrogen-bonded to Val-98β in both the oxygenated and deoxygenated states. This hydrogen bond will reduce the freedom of motion for the C-terminus of the β chain, thus stabilizing it in a conformation which may energetically facilitate re-formation of the inter-subunit salt bridges upon transition back to the T state. For Hb Phe-145β, the increase in the mobility for the C-terminus of the β subunit possibly caused by the cleavage of the hydrogen bond would destabilize the transition state, resulting in the slow R–T transition rate.

It is of interest that both of the two hydrogen bonds we focused on in the present study exert similar influences on the stabilization of the transition state, while the stabilization effects on the equilibrium T state are quite different. The difference in stabilization of the equilibrium T state is accounted for as follows. The rupture of the hydrogen bond between Tyr-145β and Val-98β is considered to be compensated by some interactions involving the benzene ring of Phe-145β in the equilibrium state, as mentioned above, whereas the hydrogen bond between Tyr-42α and Asp-99β cannot be replaced by other interactions.

In summary, the mutation at the 42α site drastically decreases the R–T transition rate and clearly shows that the hydrogen bond between Tyr-42α and Asp-99β is one of the key interactions in the R–T transition state as well as in the equilibrium T state. It is also suggested that in Hb A this hydrogen bond remains partially formed in the transition state between the R and T states and the transition state has a T-like structure as long as the subunit interface is concerned. The intrasubunit hydrogen bond between Tyr-145β and Val-98β also stabilizes the transition state, as does the hydrogen bond between Tyr-42α and Asp-99β, whereas the former shows a small contribution to the stabilization of the equilibrium T state.

REFERENCES

Andrews, P. (1964) *Biochem. J. 91*, 222–233.

Antonini, E., & Brunori, M. (1971) *Hemoglobin and Myoglobin in Their Reactions with Ligands*, North-Holland, Amsterdam.

Antonini, E., Anderson, N. M., & Brunori, M. (1972) *J. Biol. Chem. 247*, 319–321.

Baldwin, J., & Chothia, C. (1979) *J. Mol. Biol. 129*, 175–220.

Charache, S., Brimhall, B., & Jones, R. T. (1975) *Johns Hopkins Med. J. 136*, 132–136.

Chu, A. H., & Ackers, G. K. (1981) *J. Biol. Chem. 256*, 1199–1205.

Eaton, W. A., Henry, E. R., & Hofrichter, J. (1991) *Proc. Natl. Acad. Sci. U.S.A. 88*, 4472–4475.

Fersht, A. R., Shi, J.-P., Knill-Jones, J., Lowe, D. M., Wilkinson, A. J., Blow, D. M., Brick, P., Carter, P., Waye, M. M. Y., & Winter, G. (1985) *Nature (London) 314*, 235–238.

Findsen, E. W., Friedman, J. M., & Ondrias, M. R. (1988) *Biochemistry 27*, 8719–8724.

Gibson, Q. H. (1959) *Biochem. J. 71*, 293–303.

Glasstone, S., Laidler, K. J., & Eyring, H. (1941) *The Theory of Rate Processes*, McGraw-Hill, New York.

Gray, R. D. (1975) *J. Biol. Chem. 250*, 790–792.

Hofrichter, J., Sommer, J. H., Henry, E. R., & Eaton, W. A. (1983) *Proc. Natl. Acad. Sci. U.S.A. 80*, 2235–2239.

Hofrichter, J., Henry, E. R., Sommer, J. H., Deutsch, R., Ikeda-Saito, M., Yonetani, T., & Eaton, W. A. (1985) *Biochemistry 24*, 2667–2679.

Hofrichter, J., Henry, E. R., Szabo, A., Murray, L. P., Ansari, A., Jones, C. M., Coletta, M., Falcioni, G., Brunori, M., & Eaton, W. A. (1991) *Biochemistry 30*, 6583–6598.

Imai, K., Shih, D. T.-B., Tame, J., Nagai, K., & Miyazaki, G. (1989) *Protein Sequences Data Anal. 2*, 81–86.

Imai, K., Fushitani, K., Miyazaki, G., Ishimori, K., Kitagawa, T., Wada, Y., Morimoto, H., Morishima, I., Shih, D. T.-B., & Tame, J. (1991) *J. Mol. Biol. 218*, 769–778.

Ishimori, K., & Morishima, I. (1988) *Biochemistry 27*, 4060–4066.

Ishimori, K., Morishima, I., Imai, K., Fushitani, K., Miyazaki, G., Shih, D., Tame, J., Pagnier, J., & Nagai, K. (1989) *J. Biol. Chem. 264*, 14624–14626.

Ishimori, K., Imai, K., Miyazaki, G., Kitagawa, T., Wada, Y., Morimoto, H., & Morishima, I. (1992) *Biochemistry 31*, 3256–3264.

Jones, R. T., Osgood, E. E., Brimhall, B., & Koler, R. D. (1967) *J. Clin. Invest. 46*, 1840–1847.

Kaminaka, S., Ogura, T., & Kitagawa, T. (1990) *J. Am. Chem. Soc. 112*, 23–27.

Kellett, G. L. (1971) *J. Mol. Biol. 59*, 401–424.

Kellett, G. L., & Gutfreund, H. (1970) *Nature (London) 227*, 921–925.

Mathews, A. J., Rohlfs, R. J., Olson, J. S., Tame, J., Renaud, J.-P., & Nagai, K. (1989) *J. Biol. Chem. 264*, 16573–16583.

Monod, J., Wyman, J., & Changeux, J.-P. (1965) *J. Mol. Biol. 12*, 88–118.

Murray, L. P., Hofrichter, J., Henry, E. R., & Eaton, W. A. (1988) *Biophys. Chem. 29*, 63–76.

Nagai, K., Perutz, M. F., & Poyart, C. (1985) *Proc. Natl. Acad. Sci. U.S.A. 82*, 7252–7255.

Perutz, M. F. (1970) *Nature (London) 228*, 726–739.

Perutz, M. F., Fermi, G., Luisi, B., Shaanan, B., & Liddington, R. C. (1987) *Acc. Chem. Res. 20*, 309–321.

Reed, C. S., Hampson, R., Gordon, S., Novy, M. J., Brimhall, B., Edwards, M. J., & Koler, R. D. (1966) *Blood 31*, 623–632.

Sawicki, C. A., & Gibson, Q. H. (1976) *J. Biol. Chem. 251*, 1533–1542.

Sawicki, C. A., & Gibson, Q. H. (1977) *J. Biol. Chem. 252*, 5783–5788.

Sawicki, C. A., & Khaleque, M. A. (1983) *Biophys. J. 44*, 191–199.

Shaanan, B. (1983) *J. Mol. Biol. 171*, 31–59.

Sharma, V. S., Schmidt, M. R., & Ranney, H. M. (1976) *J. Biol. Chem. 251*, 4267–4272.

Schmelzer, U., Steiner, R., Mayer, A., Nedetzka, T., & Fasold, H. (1972) *Eur. J. Biochem. 25*, 491–497.

Su, C., Park, Y. D., Liu, G.-Y., & Spiro, T. G. (1989) *J. Am. Chem. Soc. 111*, 3457–3459.

Unno, M., Ishimori, K., & Morishima, I. (1990) *Biochemistry 29*, 10199–10205.

Vandegriff, K. D., Le Tellier, Y. C., Winslow, R. M., Rohlfs, R. J., & Olson, J. S. (1991) *J. Biol. Chem. 266*, 17049–17059.

Weatherall, D. J., Clegg, J. B., Callender, S. T., Wells, R. M. G., Gale, R. E., Huehns, E. R., Perutz, M. F., Viggiano, G., & Ho, C. (1977) *Br. J. Haematol. 35*, 177–191.

Wiedermann, B. L., & Olson, J. S. (1975) *J. Biol. Chem. 250*, 5283–5285.

Winslow, R. M., Swenberg, M.-L., Gross, E., Chervenick, P. A., Buchman, R. R., & Anderson, W. F. (1976) *J. Clin. Invest. 57*, 772–781.